ADVANCES IN ATMOSPHERIC SCIENCES, VOL. 33, FEBRUARY 2016, 135–150

The Impact of Cut-off Lows on Ozone in the Upper Troposphere and Lower Stratosphere over Changchun from Ozonesonde Observations

Yushan SONG[1,2], Daren LÜ[*1], Qian LI[1], Jianchun BIAN[1], Xue WU[1], and Dan LI[1]

[1]*Key Laboratory of Middle Atmosphere and Global Environment Observation, Institute of Atmospheric Physics, Chinese Academy of Sciences, Beijing* 100029

[2]*University of Chinese Academy of Sciences, Beijing* 100049

(Received 15 February 2015; revised14 June 2015; accepted 31 July 2015)

ABSTRACT

In situ measurements of the vertical structure of ozone were made in Changchun (43.53°N, 125.13°E), China, by the Institute of Atmosphere Physics, in the summers of 2010–13. Analysis of the 89 validated ozone profiles shows the variation of ozone concentration in the upper troposphere and lower stratosphere (UTLS) caused by cut-off lows (COLs) over Changchun. During the COL events, an increase of the ozone concentration and a lower height of the tropopause are observed. Backward simulations with a trajectory model show that the ozone-rich airmass brought by the COL is from Siberia. A case study proves that stratosphere–troposphere exchange (STE) occurs in the COL. The ozone-rich air mass transported from the stratosphere to the troposphere first becomes unstable, then loses its high ozone concentration. This process usually happens during the decay stage of COLs. In order to understand the influence of COLs on the ozone in the UTLS, statistical analysis of the ozone profiles within COLs, and other profiles, are employed. The results indicate that the ozone concentrations of the in-COL profiles are significantly higher than those of the other profiles between $\pm$4 km around the tropopause. The COLs induce an increase in UTLS column ozone by 32% on average. Meanwhile, the COLs depress the lapse-rate tropopause (LRT)/dynamical tropopause height by 1.4/1.7 km and cause the atmosphere above the tropopause to be less stable. The influence of COLs is durable because the increased ozone concentration lasts at least one day after the COL has passed over Changchun. Furthermore, the relative coefficient between LRT height and lower stratosphere (LS) column ozone is -0.62, which implies a positive correlation between COL strength and LS ozone concentration.

Key words: ozonesonde, cut-off low, upper troposphere, lower stratosphere, tropopause

Citation: Song, Y. S., D. R. Lü, Q. Li, J. C. Bian, X. Wu, and D. Li, 2016: The impact of cut-off lows on ozone in the upper troposphere and lower stratosphere over Changchun from ozonesonde observations. *Adv. Atmos. Sci.*, **33**(2), 135–150, doi: 10.1007/s00376-015-5054-2.

1. Introduction

The upper troposphere and lower stratosphere (UTLS) is the transition region between the troposphere and the stratosphere (e.g., Bian, 2009; Gettelman et al., 2011). The ozone controlled by stratosphere–troposphere exchange (STE) in this region plays an important role in the radiation balance and global climate change (IPCC, 1996). Brewer–Dobson circulation controls STE on the global scale, which contains upward transport through the tropopause in the tropics and downward transport in the extratropics (Brewer, 1949). Moreover, there are detailed mechanisms that significantly contribute to STE, including tropical cumulus convection, blocking anticyclones, cut-off cyclones, and tropopause folds (Holton, 1990).

Cut-off lows (COLs) are closed lows in the mid–upper troposphere that are detached from westerlies. They move slowly and usually stay in an area for several days, generally causing severe weather (Gimeno et al., 2007). A COL manifests closed isobaric contours along with a cold core or a cold trough in the synoptic chart, as well as a closed high potential vorticity (PV) center on the isentropic surface (Hoskins et al., 1985). As Nieto et al. (2005) suggested, the complete lifespan of a COL consists of four stages: (1) The upper-level trough stage: The trough forms and develops at 200 hPa, with the temperature wave behind the geopotential wave. (2) The tear-off stage: The trough deepens and detaches from the meridional stream. The air streaming into the southern region is cut off from the main flow. (3) The cut off stage: The tear-off process is complete. The COL is more pronounced. (4) Final stage: The upper-level low eventually merges back into the western flow. High PV moving with the COL from the polar to subtropical and tropical regions generally indicates the cold polar stratospheric air may intrude into the troposphere. During a COL process, there

* Corresponding author: Daren LÜ
Email: ludr@mail.iap.ac.cn

are three mechanisms that could transport stratospheric air into the troposphere (Price and Vaughan, 1993): (1) Convective erosion (e.g., Gouget et al., 2000); (2) Erosion by turbulence associated with a jet stream (e.g., Pan et al., 2007); (3) Tropopause folding near the flank of the COL (e.g., Gouget et al., 2000). This system lowers the tropopause and could eventually result in the stratosphere-to-troposphere transport (STT) (Wirth, 1995). Since PV is conservative in adiabatic and frictionless processes, a certain PV value could be chosen as the definition of the dynamical tropopause (DT) (Hoskins et al., 1985).

Ozone is well-known for its abundance in the stratosphere and dramatic decrease in concentration from the stratosphere to the troposphere. This makes ozone an effective tracer for the study of STE in COLs (Yates et al., 2013). STE controls the upper tropospheric ozone in the extratropics (Pan et al., 2004). Some STE events could even cause high surface ozone concentrations and affect air quality (Lefohn et al., 2011; Lin et al., 2012). Chen et al. (2014) used the Weather Research and Forecasting model to simulate the STE process during the lifetime of a COL. A diagnostic formula was used to calculate the cross-tropopause mass flux (both horizontal and vertical transport) during the COL's development. They found that during the whole lifetime of a COL, the effect of horizontal transportation is dominated by STT, while the vertical transportation can be attributed to the troposphere-to-stratosphere transport (TST). The STE on the western side of the trough and moving COL is dominated by STT, and STE on the eastern side of the trough is dominated by TST. The net mass transportation induced by a COL is STT. Liu et al. (2013) used ozone data from satellite measurements along with reanalysis data to study the effect of stratospheric intrusion on column ozone and ozone profiles during a COL, and suggested that there is stratospheric intrusion at the rear of a COL.

Ozone data can be obtained from satellite, lidar, ozonesonde and aircraft measurements, as well as reanalysis data. Reanalysis data have been used frequently in previous studies of STE, especially in model-based studies (Yang and Lü, 2003; Zhang et al., 2010; Liu et al., 2013; Chen et al., 2014). Satellite observations are another data source for STE studies (Barré et al., 2012; Liu et al., 2013). However, the vertical resolution and accuracy (especially in the troposphere) of ozone observations still need further improvement. Therefore, ozonesonde and aircraft measurements are highly valuable because of their finer vertical resolution and better quality, and are thus usually employed to evaluate satellite data (Bian et al., 2007; Pittman et al., 2009) and model performance (Logan, 1999a, 1999b; Tilmes et al., 2012). A number of ozonesonde and aircraft launches have been conducted regularly at certain sites for many years (Kim and Lee, 2010; Ganguly and Tzanis, 2011; Srivastava et al., 2012; Wang et al., 2012), while others have lasted for several days or months at one or more site, sometimes in conjunction with aircraft and lidar measurements (Oltmans et al., 1996; Kuang et al., 2012; Ojha et al., 2014). Benefiting from the high resolution of ozone profiles in the UTLS, ozonesonde data are very useful for analyzing the role of STE in tropospheric ozone variation (Ganguly and Tzanis, 2011; Ojha et al., 2014) and describing the process of stratospheric intrusion (Li et al., 2015). However, due to a lack of data for a statistical study of STE, ozonesonde data are often used in case study analyses (Oltmans et al., 1996; Cui et al., 2004; Li et al., 2015).

The Key Laboratory of Middle Atmosphere and Global Environment Observation, Institute of Atmospheric Physics (IAP), Chinese Academy of Sciences, conducted a field campaign of observations over Changchun (43.53°N, 125.13°E), China, in the summers of 2010–13, by using ozonesondes developed at the IAP. Changchun is located in the northeast of China where COLs occur frequently in summer (e.g., Hu et al., 2010). The measurements lasted about one month, around June, in each year. During each observation period, several COLs were detected, and a number of case studies based on this dataset have already been published (Chen et al., 2014; Li et al., 2015), mainly discussing the STE in the different stages of a COL that occurred during 19–23 June 2010. Benefiting from this dataset, the possibility exists to statistically investigate the effect of COLs on the ozone vertical distribution, reaching more general conclusions than is achievable through individual case studies. Accordingly, in this paper, the vertical distribution of ozone concentration over Changchun is presented. Section 2 describes the data and method used. Section 3 discusses the variation of the ozone concentration and its response to COLs, by a case study and statistical analysis. Finally, section 4 summarizes the results.

2. Data and method

2.1. *Ozonesonde measurements*

The IAP launched balloons equipped with an ozonesonde and radiosonde in Changchun at around 1400 LST (local solar time) every day during the observation periods. There were also a handful of measurements taken at around 0000 LST. The observation times were 26 May to 26 June 2010, 1–30 June 2011, 9 June to 15 July 2012, and 28 May to 30 June 2013. Besides ozone, other parameters including temperature, relative humidity, wind speed, and wind direction were obtained at the same time.

The instrument adopted during observations from 2010 to 2012 was the single-cell Global Positioning System ozonesonde sensor (GPSO3), developed by the IAP (Wang et al., 2004a, 2004b; Xuan et al., 2004). GPSO3 is an electrochemical sensor, similar to the Electrochemical Concentration Cell (ECC) ozonesonde (Komhyr et al., 1995). In 2001, parallel observations by GPSO3 and a Vaisala ECC sensor were taken in Beijing (Xuan et al., 2004). The results showed that the performance of GPSO3 is similar to the Vaisala sensor. The correlation coefficient between the GPSO3 and Vaisala ECC sensor profiles was 0.988. Meanwhile, the ratio of total column ozone from GPSO3 and Dobson ozone spectrometer measurements was 1.0588, on average. The authors concluded that the GPSO3 sensor is reliable. Parallel launches of GPSO3 and a Vaisala ECC sen-

sor were also conducted in 2005, and comparison showed the ozone variability in the UTLS region from the GPSO3 sensor to be consistent with that from the Vaisala ECC sensor (Bian et al., 2007). We revised the ozone profiles of 2010–12 based on the pump efficiency coefficient of the GPSO3 ozonesonde indicated by Xuan et al. (2004). In 2013, the single-cell sensors were upgraded to a double-cell type called the "IAP ozonesonde" (Zhang et al., 2014a). A preliminary validation has shown that the relative difference between the IAP and Vaisala ozonesondes is 4.9% (Zhang et al., 2014b).

The present study focuses on the variation of the ozone concentration in the UTLS. Due to some unexpected circumstances, such as the balloon bursting too early, the electrodes of the electrochemical cell diffusing, and loss of signal when entering thunderclouds, some of the ozone profiles are incomplete in the UTLS. Therefore, only those profiles that contain complete ozone information in the UTLS (defined in this study as ranging from 4 km below the tropopause to 4 km above) were selected. Accordingly, the number of effective profiles is 28 in 2010, 33 in 2011, and 28 in 2012.

2.2. *Methodology*

The COL is usually detected by closed geopotential contours at 500 hPa, 300 hPa, or 200 hPa (Kentarchos and Davies, 1998; Yang and Lü, 2003; Hu et al., 2010). The COLs detected at 500 hPa in northeastern China, which can cause severe weather at the surface, are called "northeast cold vortexes" (Sun et al., 1994). The level of 200 hPa is around the tropopause and is a crucial diagnostic for STE processes. Here, we detected COLs at 500 hPa, 300 hPa, 250 hPa, and 200 hPa according to the time of 89 ozone profiles. We analyzed European Centre for Medium-Range Weather Forecasts (ECMWF) Interim Reanalysis (ERA-Interim) data with a horizontal resolution of $0.25^\circ \times 0.25^\circ$ and temporal resolution of four times per day (0200, 0800, 1400, 2000 LST) to detect COLs in the synoptic charts. The criterion of COL detection applied was to recognize the closed contours of geopotential height. To investigate the impact of COLs on the ozone concentration in the UTLS, ozone profiles were classified into two types according to the COLs at a certain level: profiles in COLs and other (normal) profiles (see section 3.3).

To trace the origin of air parcels in COLs, we used the Hybrid Single Particle Lagrangian Integrated Trajectory (HYSPLIT) model (Draxler and Rolph, 2003) and Global Data Assimilation $1^\circ \times 1^\circ$ dataset reprocessed from the National Centers for Environmental Prediction, provided by the National Oceanic and Atmospheric Administration (NOAA) Air Resources Laboratory, to calculate the back trajectories of air masses in Changchun for two cases.

In previous studies, there have been various definitions of the tropopause, such as the thermal definition (WMO, 1957), dynamical definition (Danielsen et al., 1987), and ozone definition (Bethan et al., 1996). The DT, defined by a certain PV value, is regarded as a material surface in adiabatic and frictionless processes, making it a good choice for the study of STE (Hoskins et al., 1985; Bian, 2009). In this case, however, the DT calculated from reanalysis data may not match that calculated from sonde data due to the huge gap in resolution between them. In our campaigns, the balloon-borne radiosonde measured temperature profiles at the same time. The thermal tropopause calculated from the temperature profiles will agree well with observed ozone and precisely reveal the condition of the air's static stability. Pan et al. (2004) indicated that the tropopause in the extratropics is a transition layer that is centered on the thermal tropopause, which implies that the thermal tropopause could roughly distinguish between the troposphere and stratosphere from the chemical perspective. In this paper, the lapse-rate tropopause (LRT) is calculated based on the radiosonde temperature profiles (WMO, 1957). The first LRT is defined as the lowest altitude at which the temperature lapse rate decreases to 2°C km^{-1}; and the temperature lapse rate of any point within the next 2 km above from the first tropopause should not exceed 2°C km^{-1}. To avoid boundary layer inversions, the tropopause height should be calculated above the level of 500 hPa (Homeyer et al., 2010). If there is a certain level above the first tropopause, provided the lapse rate of any level within the next 1 km above from this level exceeds 3°C km^{-1}, then, the second tropopause can be calculated at the altitudes above that certain level by using the criterion of the first tropopause. To minimize the temperature discretization-induced noise in the tropopause calculation, 100 m sampling of temperature profiles was applied (Homeyer et al., 2010). We identified the profiles with the first LRT larger than 15 km as tropical profiles, and the others as subtropical profiles (Randel et al., 2007).

The DT was calculated using PV data from the ERA-Interim dataset. The altitudes between the 1000 hPa and 1 hPa level were divided into 37 levels. Bourqui (2006) calculated the STE in a COL event with the DT definition within 1.5 to 5 PVU, suggesting that the STT pattern during the COL decay stage occurs only when the PV value of DT is less than 4 PVU. We applied 1, 1.5, 2, 2.5, 3, 3.5 and 4 PVU to calculate the DT (figures are not shown). It was found that 3.5 PVU DT agrees well with the LRT tropopause (shown in section 3.1). Therefore, we chose the 3.5 PVU isosurface as the DT.

The mean and standard deviation are provided to compare the ozone profiles from different groups. The probability distribution functions (PDFs) of ozone were also calculated, to characterize the ozone distribution. Besides, we applied the Hellinger distance (Nikulin, 2001; Tilmes et al., 2012) to describe the similarity between two distributions. $P = (p_1, p_2, \ldots p_k)$, $Q = (q_1, q_2, \cdots q_k)$ are two probability measures of ozone partial pressure. Their Hellinger distance is defined as

$$H(P,Q) = \frac{1}{\sqrt{2}} \sqrt{\sum_{i=1}^{k} (\sqrt{p_i} - \sqrt{q_i})^2}.$$

$H(P,Q)$ satisfies the property $0 \leqslant H(P,Q) \leqslant 1$. A Hellinger distance (HD) of 0 indicates the two distributions are identical, while an HD of 1 indicates they are completely different (Tilmes et al., 2012).

2.3. *Comparison between Changchun and Sapporo ozone profiles*

To validate the ozone profiles in Changchun in May, June and July from 2010 to 2012, we compared the observations between Changchun (43.53°N, 125.13°E), China, and Sapporo (43.1°N, 141.3°E), Japan (Fig. 1). Table 1 displays the launch dates in Changchun and Sapporo. The ozone profiles in Sapporo from 2010 to 2012 were measured using an ECC ozonesonde, which is known for its mature technology. Sapporo ozonesonde data can be obtained from the World Ozone and Ultraviolet Radiation Data Centre (WOUDC) website (http://www.woudc.org/). The vertical ozone structures of the two sites are similar, with an ozone peak at the height of 24 km above Changchun and 23 km above Sapporo. Between the layers of 10 km and 18 km, the ozone concentration in Changchun is higher than that in Sapporo and there appears to be a slight secondary ozone peak. Below 13 km, Changchun's ozone concentration greatly exceeds that in Sapporo, with the difference even exceeding 80% near the surface. The high tropospheric ozone concentration in Changchun may result from photochemical production.

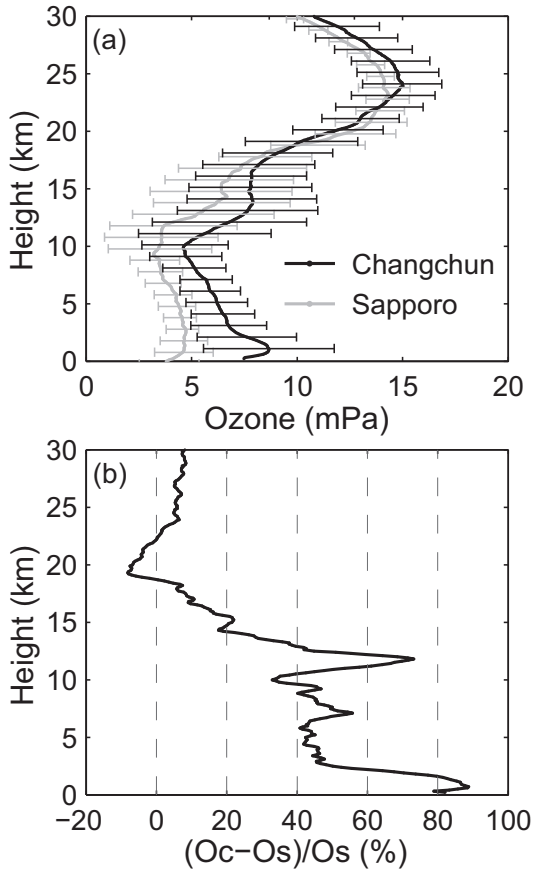

Fig. 1. (a) Comparison of the mean ozone profile between Changchun (black line) and Sapporo (grey line) in May, June and July from 2010 to 2012. The thick line is the mean profile and error bars show $\pm\sigma$ from the mean. (b) Relative difference between Changchun and Sapporo, computed as follows: (Changchun–Sapporo)/Sapporo.

Table 1. Local launch times at Changchun and Sapporo. Changchun (Sapporo) local time equates to UTC time offset by eight (nine) hours.

	2010		2011		2012	
Station	Date	Time	Date	Time	Date	Time
Changchun	5/26	14:06	6/1	15:00	6/9	13:55
	5/27	14:01	6/2	14:23	6/10	13:58
	5/29	14:06	6/3	14:09	6/11	13:58
	5/30	13:49	6/4	14:05	6/12	13:57
	5/31	14:08	6/5	13:52	6/14	14:16
	6/1	13:48	6/7	00:05	6/17	14:16
	6/2	14:04	6/7	14:13	6/18	14:03
	6/3	14:03	6/8	14:10	6/19	13:55
	6/6	14:09	6/9	00:05	6/20	14:12
	6/7	13:55	6/9	14:47	6/22	14:12
	6/8	13:52	6/10	00:04	6/23	14:09
	6/9	13:51	6/10	14:09	6/24	14:01
	6/10	13:53	6/11	00:07	6/25	14:05
	6/12	13:44	6/12	00:12	6/26	14:04
	6/13	13:56	6/12	14:05	6/28	14:08
	6/15	13:53	6/13	14:20	6/30	14:15
	6/16	13:55	6/14	00:16	7/1	14:16
	6/17	13:58	6/14	14:05	7/2	14:16
	6/18	14:01	6/15	14:04	7/3	14:00
	6/20	13:54	6/16	14:13	7/4	14:09
	6/21	00:01	6/17	14:08	7/5	14:20
	6/22	00:01	6/18	14:13	7/9	14:11
	6/22	13:59	6/19	14:14	7/12	00:02
	6/23	00:02	6/20	14:05	7/12	14:13
	6/23	13:59	6/21	14:24	7/13	00:01
	6/25	00:09	6/22	14:06	7/14	14:39
	6/26	00:02	6/23	14:15	7/15	00:07
	6/26	14:03	6/24	14:12	7/15	14:12
			6/26	14:27		
			6/27	16:28		
			6/28	14:21		
			6/29	14:09		
			6/30	14:08		
Sapporo	5/17	14:30	5/9	14:31	5/1	14:30
	6/10	14:30	5/18	15:24	5/17	14:30
	6/30	14:37	5/26	14:30	5/24	15:11
	7/15	14:52	6/7	14:34	6/4	14:30
			6/29	14:39	6/13	14:31
			7/6	14:45	6/19	14:30
			7/11	14:30	6/26	14:49
			7/20	14:30	7/4	14:30
			7/28	14:45	7/13	14:35
					7/18	14:30
					7/23	14:30
					7/30	14:30

Based on previous studies (Mauzerall et al., 2000; Fishman et al., 2003), the tropospheric ozone production and residual in Changchun are higher than those in Sapporo in boreal summer. In general, the GPSO3 ozonesonde seems to overestimate the ozone concentration in the troposphere and bottom layer of the stratosphere. Xuan et al. (2004) concluded that the mean total ozone measured by the GPSO3 ozonesonde is larger than that measured by the Dobson ozone spectrome-

ter. However, the total ozone measured by the Vaisala ECC ozonesonde is less than that measured by the Dobson ozone spectrometer, which implies that GPSO3 may overestimate the ozone concentration while ECC may underestimate it (Xuan et al., 2004). To investigate the difference of ozone in the ULTS region, the PDF of ozone at 12–15 km for Changchun and Sapporo are presented in Fig. 2a. The HD of the ozone distributions between Changchun and Sapporo (0.26) implies that the ozone in the lower stratosphere is distributed similarly at the two stations, but also features some different characteristics. Figure 2a shows that most ozone partial pressures at Sapporo are between 1 mPa and 10 mPa, with a peak at 2 mPa. Meanwhile, the ozone PDF for Changchun shows a bimodal structure that spans between 2 mPa and 13 mPa, with peaks at 3 mPa and 9 mPa. The air masses with low ozone partial pressure (2 mPa) and high ozone partial pressure (9 mPa) are associated with air from low and high latitudes, respectively (Logan, 1999a). This infers that, during the observations, Changchun was more influenced, compared to Sapporo, by air from higher latitudes. In subtropical areas, the thermal tropopause breaks near the jet stream (Gettelman et al., 2011). If a station is situated in the south/north of the jet stream, the thermal tropopause will be similar to a tropical/polar tropopause. Figure 2b shows most LRT heights to be lower than 14 km, both in Changchun and Sapporo, meaning both stations feature a subtropical tropopause. Sapporo has a larger tropopause PDF at around 15 km, implying that Sapporo is more strongly influenced by tropical mass. The PDF of the LRT height for Sapporo has a narrow peak at around 12 km and 13 km. In contrast, the PDFs spread from 10 km to 13 km in Changchun. This proves that polar air masses with high ozone concentrations and a lower tropopause contribute high values in the UTLS of Changchun ozone profiles, which could result from COLs controlling the station or the jet stream moving southward.

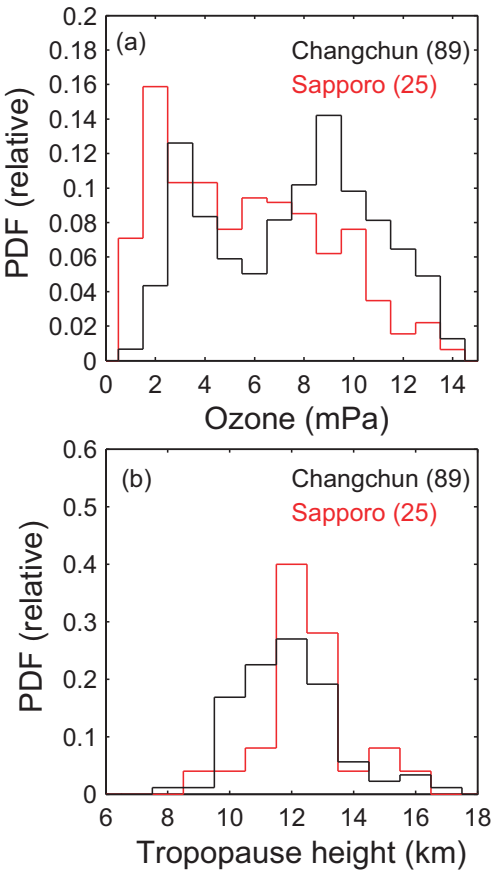

Fig. 2. (a) PDF of ozone at 12–15 km in Changchun and Sapporo. The HD of ozone distributions is 0.26. The number of profiles from Changchun and Sapporo is 89 and 25, respectively. (b) PDF of tropopause height (LRT) at each station. The HD of the LRT distribution is 0.28.

3. Results and discussion

3.1. *UTLS ozone distribution and variation*

The time–height cross sections of ozone in Fig. 3 show all of the ozone vertical distributions in the UTLS over Changchun during the observations in the three-year study period. Most of the DTs are consistent with the first LRTs, except on those days with a tropical tropopause (e.g., 29 June 2011, 9 July 2012). On 9 July 2012, the LRT over Changchun was 16.5 km, but the DT was 11.6 km. In fact, the lapse rate of temperature was less than 2°C km^{-1} above 11.5 km, but this level could not strictly satisfy the first LRT definition (lapse rate of any point within the next 2 km above the first tropopause should not exceed 2°C km^{-1}). In static stability cross sections, this usually shows an LRT break in the latitude near the jet. On the anticyclonic side of the jet, the tropopause breaks, which could result in the LRT altitude being higher than the DT altitude (e.g., Pan et al., 2007, Fig. 5a). The tropopause acts like a barrier, separating the high ozone concentration in the stratosphere from the low ozone concentration in the troposphere. The heights of Changchun's LRTs were from 7.9 km to 16.6 km, with an average of 12.0 km. When stratospheric air with a high ozone concentration subsides into the low altitudes, the tropopause height also decreases (e.g., 29 May and 21 June 2010; 3 June 2011; 11 and 18 June 2012). Such stratospheric subsiding results in a second ozone peak around the tropopause in the ozone vertical profiles, and thus the Changchun ozone profiles generally show a double-peak structure. In Fig. 1a there is also a slight ozone spike between 10 km and 16 km in the mean ozone profile of Changchun. Moreover, Fig. 3 shows the signal of ozone seasonal variation. The ozone concentration in the UTLS is lower in late June and July than in early and mid-June. This agrees with the finding of Xie and Cai (2000) that total ozone in East Asia shows approximate sinusoidal variation in a year, with a maximum in May and a minimum in October. Considering the tropical tropopause is associated with tropical air masses with lower ozone concentrations (Logan, 1999a), we divided all the ozone profiles into two groups: profiles with a tropical LRT, and those with a subtropical LRT. Figure 4a shows the PDFs of ozone at 1–3 km above the first LRT altitude, for both groups. The difference be-

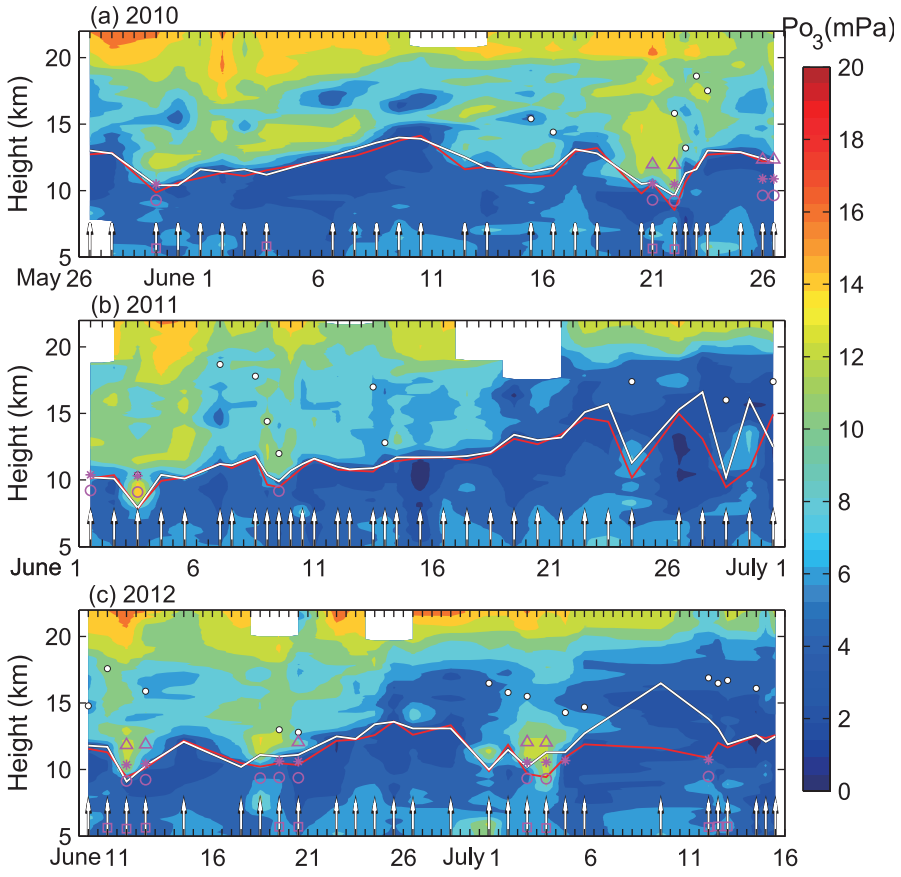

Fig. 3. Time–height cross sections of ozone at Changchun in (a) 2010, (b) 2011 and (c) 2012. The time axes are split into two times per day, in which the first measurement was taken at midnight, local time (∼0000 LST), and the second in the afternoon (∼1400 LST). The measurements taken at midnight were few in number. The white solid lines and white dots display the first and second LRTs derived from the temperature profiles. The red lines mark the DT defined by 3.5 PVU. The white arrows along the time axis mark the launch time of the ozonesonde. The magenta squares, circles, asterisks and triangles represent the COLs over Changchun detected at 500 hPa, 300 hPa, 250 hPa and 200 hPa, respectively.

tween the distributions is significant, with an HD of 0.62. The ozone partial pressure for a tropical LRT is between 3 mPa and 8 mPa, with the PDF peak at 4 mPa. But the ozone partial pressure for a subtropical LRT is mainly distributed between 7 mPa and 13 mPa, with a peak at 9 mPa. Therefore, in late June and July, the low ozone concentration accompanying the higher tropopause is influenced by tropical air masses, which could be caused by the jet stream moving northward. On the other hand, the double-peak structure in the ozone profiles could be influenced by polar air masses with high ozone concentrations. The air mass properties over Changchun are associated with the changing location of the jet stream. Pan et al. (2009) suggested that tropospheric intrusions associated with the secondary tropopause are characterized by low ozone concentrations. To investigate the influence of double tropopauses, all the ozone profiles with subtropical LRTs were divided into two groups: double LRTs and single LRTs (Fig. 4b). The HD of the ozone distributions (0.21) implies that the difference between the two groups is not sufficiently distinct. Over Changchun, a double tropopause can not only be induced by tropospheric intrusion, but also by stratospheric intrusion along with tropopause folding. The two mechanisms bring opposite influences on ozone in the UTLS and counteract one another.

Of the 89 observations over Changchun, COLs occurred in 21 (magenta markers represent COLs in Fig. 3). The COLs at 300 hPa (magenta circles) match all of the stratospheric subsidence events, and the COLs usually accompany a lower tropopause and higher ozone concentration above the tropopause. Therefore, we deduced that such intensive stratospheric air subsidence and secondary ozone peaks in the ULTS are caused by COLs.

Li et al. (2015) analyzed the entire process of a COL that occurred over East Asia, around Changchun, during 19–23 June 2010, and discussed the origin of the air mass in the COL. The air parcel with the highest ozone concentration in the center of the COL was traced back to Siberia. During the tear-off stage of the COL, high-ozone air from the polar

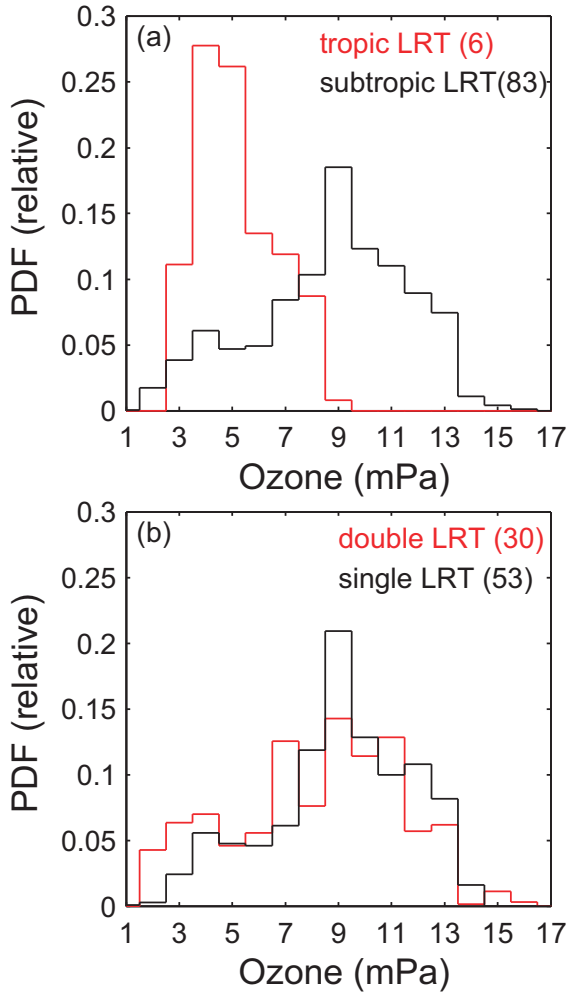

Fig. 4. (a) PDFs of ozone at 1–3 km above the first LRT altitude for the profiles with a tropical LRT (>15 km) and with a subtropical LRT (⩽15 km). The HD of the tropical and subtropical profiles is 0.62. (b) PDFs of ozone at 1–3 km above the first LRT altitude for the subtropical profiles with double LRTs and with a single LRT. The HD of double and single LRTs is 0.21. The number of profiles for each group is shown in brackets behind the name of group.

ozone reservoir was transported equatorward. When the COL reached Changchun, the air from a subpolar vortex brought high ozone concentrations above the tropopause. This is also presented in Fig. 3. Figure 5a displays the back trajectories for a typical COL, which occurred on 2 July 2012. This COL derived from East Siberia (62°N, 114°E). The trajectories indicate that the air parcels around the tropopause can be traced back to latitudes higher than 55°N. The trajectory path with cyclonic curvature illustrates that a high-ozone mass was conveyed from Siberia to Changchun by the COL. However, as Li et al. (2015) analyzed, there are various sources of air masses in COL. In fact, COLs carry both high- and low-ozone air. For example, on 12 July 2012, a COL was detected at 500 hPa, 300 hPa and 250 hPa, but the ozone concentration around the tropopause showed no obvious change (Fig. 3c). At the same time, the tropopause height was 13.8 km, which was higher than the tropopause in other COLs. Synoptic patterns at 300 hPa show that this COL formed in the east of Mongolia (48°N, 113°E) at 2000 LST 9 July 2012, then traveled eastward until reaching Changchun (43.53°N, 125.13°E) at 1400 LST 11 July 2012 (the isobaric charts are not shown). The thermal tropopause lifted when the COL was in the decay stage at 0000 LST 12 July. A similar phenomenon has also been discussed in a cut-off case by Li et al. (2015). Compared to other COLs, this one set out at a relatively low latitude and basically moved with the westerly flow. This COL system carried air with a high ozone concentration from high latitudes (48°N) and air with a low ozone concentration from the westerly flow. The latter is comparable to the ozone concentration of Changchun. Our ozonesonde observations indicate that, coincidentally, Changchun is influenced by the ozone from westerlies. This analysis is supported by the back trajectories shown in Fig. 5b, which reveal that the air parcels around the tropopause at Changchun arrived with the westerlies, and the trajectories are all situated south of 45°N. The different areas of origin of the air parcels in two cases explain the difference of Changchun's ozone concentration in the UTLS between 2 and 12 July 2012 (Fig. 3c). This special case on 12 July 2012 suggests that single-station measurements may sometimes not be able to capture the entire process of the COL. The formation and transport mechanism of a COL, as well as the location of the observation, both influence the ozone observations.

3.2. *The impact of COLs on UTLS ozone: a case study*

The stratospheric ozone that intruded on 3 July 2012 represents a slightly different case compared to others, because the high ozone concentration penetrated across the LRT. Figure 6 shows the synoptic charts, with tropopause height shaded, for 1 to 4 July 2012. The corresponding ozone partial pressure, ozone mixing ratio and static stability profiles are presented in Fig. 7. On 1 July, the COL was located to the northwest of Changchun (Fig. 6a). There was a low-tropopause center moving with the COL, where the tropopause height decreased to 9 km. As shown in Fig. 7a, the ozone partial pressure peak around the LRT (11.5 km) was only 8.4 mPa at 12.7 km. The static stability increased from 3.9×10^{-5} s^{-2} below the tropopause to 7.2×10^{-4} s^{-2} above the tropopause. Both the ozone mixing ratio and the stability in the troposphere were smaller than those in the stratosphere. On the following day, the COL centered at Changchun and dipped the LRT to 10.2 km, and the ozone peak increased to 13.4 mPa at 11.1 km (Fig. 7b). The ozone mixing ratio in the lower stratosphere was also larger than that on the former day. There was an abrupt increase from the troposphere to the stratosphere in the ozone mixing ratio profile, meaning the tropopause still clearly separated the troposphere and stratosphere from the chemical perspective. It is interesting that, on 3 July, the tropopause over Changchun recovered to 11.3 km, even though the COL still controlled Changchun. The ozone partial pressure in the UTLS was still very high, with a peak of 13.4 mPa at 9.8 km (Fig. 7c). The static stability on 2 July increased sharply at 10.2 km and reached 5.5×10^{-4}

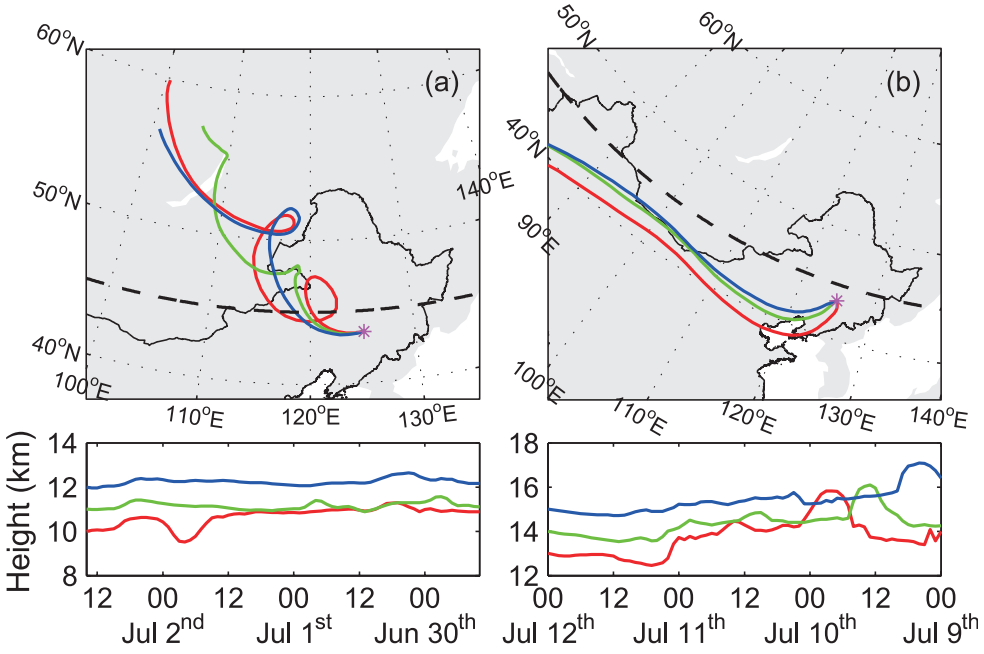

Fig. 5. Three-day trajectories from Changchun at (a) 1400 LST 2 July 2012 and (b) 0000 LST 12 July 2012. The black dashed lines mark 45°N. The LRT height over Changchun is 10.2 km at 1400 LST 2 July and 13.8 km at 0000 LST 12 July. The red, green and blue lines in (a) represent the trajectories from Changchun at the heights of 10 km, 11 km and 12 km, respectively. (b) Trajectories at the heights of 13 km, 14 km and 15 km.

s^{-2} at 10.5 km, but the stability on 3 July was smaller relative to 2 July and only reached 3.7×10^{-4} s^{-2} at 10.5 km. This indicates that, on 3 July, the high-ozone air mass stayed at around 10 km, while the thermal property of this mass became unstable. This means that the air mass possessed both the stratospheric chemical and tropospheric thermal characteristics. On 3 July, the DT was only 9.4 km, 1.9 km lower than the LRT. As Birner et al. (2002) indicated, the DT is significantly lower than the LRT in cyclones. The DT is defined by a certain value (3.5 PVU in this study):

$$\mathrm{PV} \approx \rho^{-1} \zeta_a \frac{\partial \theta}{\partial z} ,$$

$$N^2 = \frac{g}{\theta} \frac{\partial \theta}{\partial z} .$$

Therefore, PV is proportional to the vorticity (ζ_a) and static stability (N^2). An increase in ζ_a would cause a decrease in static stability around the DT height in the COL system, to keep PV constant. On the other hand, the LRT is only related to static stability. A decrease in static stability around the DT makes this level unstable, and thus lifts the LRT's altitude. Due to the instability in the UTLS on 3 July, the thermal tropopause was not definite, and failed to block the transport between the troposphere and stratosphere. The ozone concentration was gradually distributed around the tropopause. This supports the conclusion in Pan et al. (2007), that the pronounced ozone transition is related to the definite thermal tropopause. All of the above indicates the occurrence of transport from the stratosphere to the troposphere on 3 July. This phenomenon usually happens in the decay stage of a COL, as suggested by previous studies (Wirth, 1995; Li et al., 2015). Afterwards, the COL continued to get weaker, and the ozone peak around the tropopause recovered to 10.3 mPa on 4 July. When the COL moved away from Changchun, the UTLS ozone returned to the pattern of 1 July. In this case, a COL from Siberia brought high-ozone mass to the UTLS over Changchun and caused the height of the tropopause to decrease. Eventually, the stratospheric air, with high-concentration ozone, turned into tropospheric air. At the same time, the tropopause reformed at higher altitudes. These profiles actually sketch a complete STT process imposed by a COL and support the former description about STE during the decay stage of COLs.

3.3. *The impact of COLs on UTLS ozone: statistical analysis*

Figure 3 shows that most COLs cause the UTLS ozone concentration to increase. To quantitatively demonstrate this viewpoint, the profiles with a subtropical LRT are classified into two types (profiles in COLs and other profiles), to study the impact of COLs. The profiles impacted by tropical air mass have been removed because of the large difference in ozone between the tropical and subtropical profiles in Fig. 4a. As mentioned in section 3.1, the COL case around 12 July 2012 was an exception, because the COL did not bring high ozone to the UTLS. Therefore, here, we do not classify the profiles on those days as profiles influenced by COLs, and only investigate the increase of ozone concentration in the UTLS induced by COLs. In Fig. 8, the height coordinate relative to the LRT and DT removes the variation of tropopause

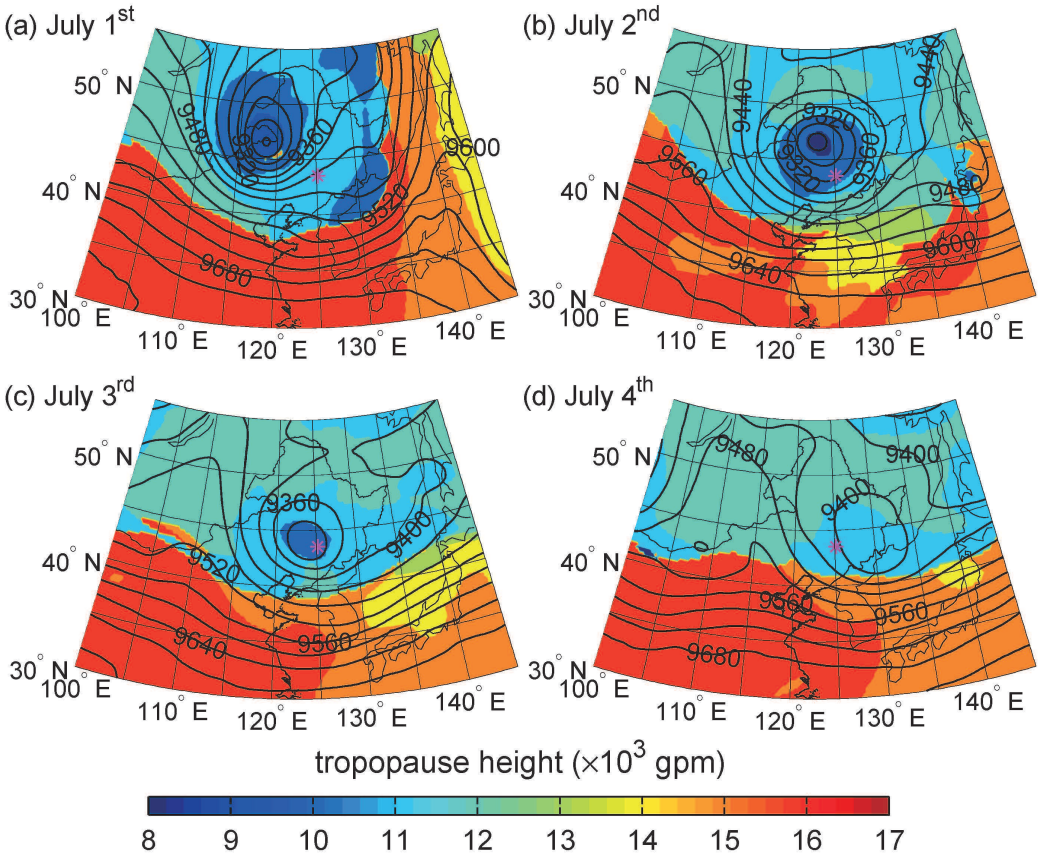

Fig. 6. ERA-Interim geopotential height (contours) and LRT height (shading) fields at 300 hPa during a cut-off low process on (a) 1 July, (b) 2 July, (c) 3 July, and (d) 4 July 2012. The LRT heights are retrieved from ERA-Interim temperature profiles.

height and focuses on the UTLS region. Birner et al. (2002) introduced this coordinate, which is also convenient for our study of chemical STE. All of the four levels (500 hPa, 300 hPa, 250 hPa, and 200 hPa) reveal that the ozone concentration in the UTLS of the in-COL profiles is higher than that of the other profiles. The mean tropopause (both LRT and DT) height of in-COL profiles is lower than that of the other profiles. In Fig. 3, we find that the COLs shown at 300 hPa correspond well with stratospheric subsidence. The COLs lower the LRT height by an average of 1.4 km, and the DT height by 1.7 km. The results with the LRT coordinate and DT coordinate are similar. In Fig. 8b, there is a significant difference between the two types of profiles from 4 km below the tropopause to 4 km above it. These results reveal that COLs (detected at 300 hPa) may cause the ozone concentration to increase significantly in the UTLS. At 1.5 km above the tropopause, the difference between the two types of profiles reaches 2.9 mPa, meaning COLs cause the ozone partial pressure to increase by 33%. The average UTLS column ozone (between 4 km below and above the LRT) is 76.2 DU for the profiles in COLs, and 57.8 DU for other profiles. This indicates that COLs cause UTLS column ozone to increase by 32%. Besides, the ozone concentration in the lower stratosphere (LS) increases by 33%, more than that (29%) in the upper troposphere (UT). As illustrated in Fig. 5a, the high ozone mass is transported from high latitudes almost at the same height. Thus, most of the increased ozone concentrations in the UT and LS over Changchun come from the troposphere and the stratosphere, respectively. The larger increase in the LS is consistent with the higher ozone concentration in the stratosphere. There is also air with a high ozone concentration penetrating through the obstacle of the tropopause, e.g., the case on 2 July 2012. However, the contribution of that case is less visible in Fig. 8. Although at all of the four levels the in-COL profile displays a higher ozone concentration in the UTLS compared to the other profiles, there are slight differences. At 200 hPa, COLs were only detected nine times during our measurements. Moreover, the gap between the two types of profiles and the difference in the two mean tropopause heights are least. Figure 8 implies that COLs over Northeast China are deep systems that perform distinctly at the levels between 500 hPa and 250 hPa, causing the ozone concentration to increase at the heights between $\pm$4 km relative to the tropopause within the systems. If COLs are recognized at 500 hPa, the gap between the two composite profiles is the largest. But some events are neglected at 500 hPa, such as that of 3 June 2011 (Fig. 3b). We find that the 300 hPa level not only performs best in terms of detecting COLs, but also in

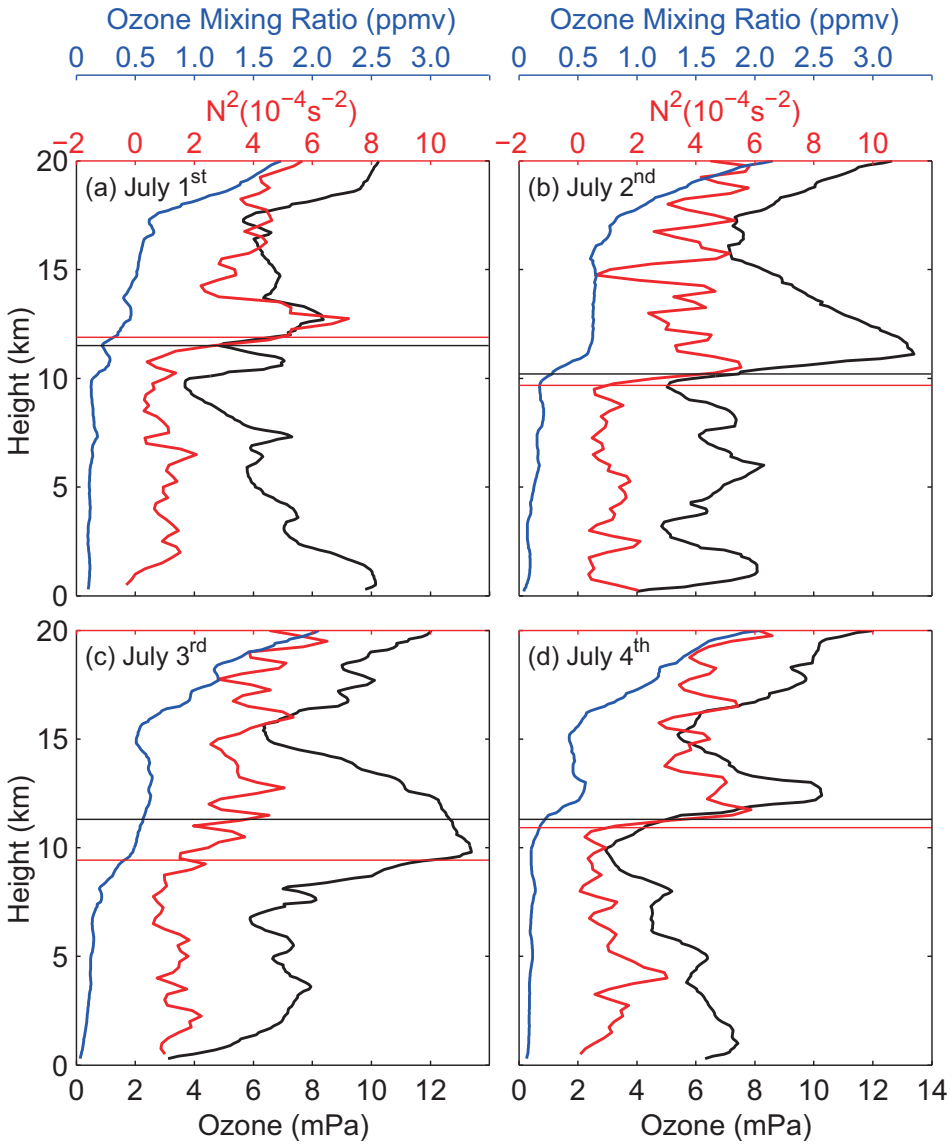

Fig. 7. Ozone partial pressure (black), ozone mixing ratio (blue) and static stability parameter buoyancy frequency N^2 (red) profiles for (a) 1 July, (b) 2 July, (c) 3 July, and (d) 4 July. Horizontal black lines mark the LRTs on 1, 2, 3 and 4 July with heights of 11.5 km, 10.2 km, 11.3 km and 11.3km, respectively. Horizontal red lines mark the DTs with heights of 11.9 km, 9.7 km, 9.4 km and 10.9 km, respectively.

distinguishing between the two types of profiles. Therefore, the following COL detection and profile classifications were both made at 300 hPa. Figure 9 displays the different ozone distributions between in-COL profiles and other profiles at 1–3 km above the first LRT and DT. In Fig. 9a, the ozone at 1–3 km above the LRT from profiles not in COLs is distributed from 2 mPa to 13 mPa, with a peak at 9 mPa. In contrast, the ozone from profiles in COLs is mostly distributed in a narrow range between 9 mPa and 13 mPa, with a peak at 13 mPa. This shows an increase of ozone in the lower stratosphere caused by the COLs. In the DT coordinate shown in Fig. 9b, the distribution of lower stratospheric ozone in the COLs has a peak at 9 mPa, whereas the distribution of ozone not in the COLs has a peak at 13 mPa. The PDFs in the DT coordinate are quite similar to the results in the LRT coordinate. The HD value is 0.47 and 0.48 for the LRT and DT coordinate, respectively, proving that the change caused by the COLs is great. Figure 10a illustrates the static stability profile of two conditions (in COLs and the other profiles, also in the coordinate relative to the LRT). Note that there is a sharp discontinuity around the tropopause in both types of profiles, which could be proof that the thermal definition we chose successfully delineates the tropopause as a barrier between the stratosphere and troposphere. The structures of the buoyancy frequency (N^2) profiles agree with results for the extratropics in previous studies (Birner et al., 2002; Pan et al., 2004; Gettelman et al., 2011). N^2 is smaller in in-COL profiles than normal profiles at 0–2 km above the tropopause. The maximal static

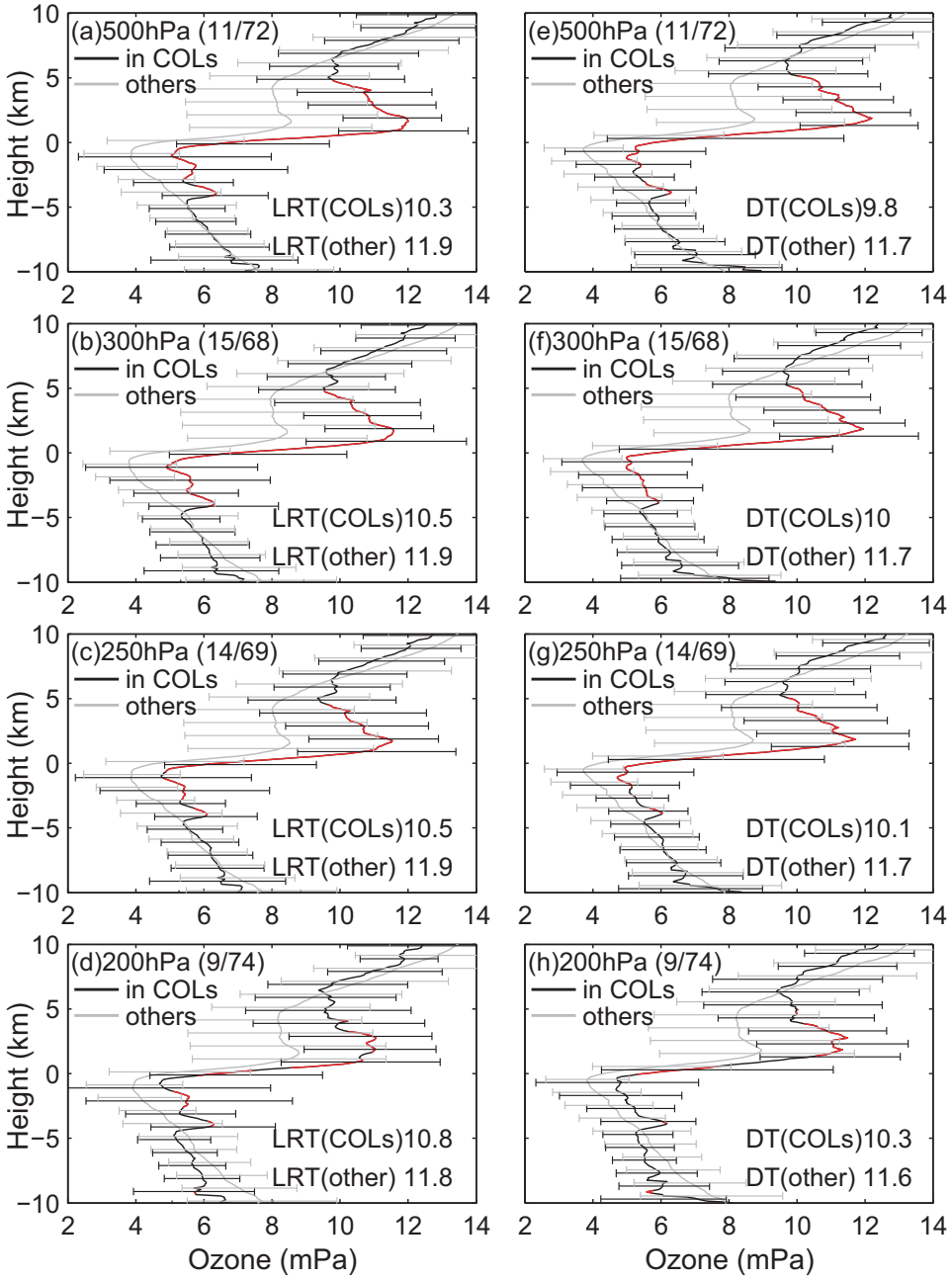

Fig. 8. Composite ozone profiles in the coordinates of height relative to the LRT height and DT height. Only those profiles with subtropical LRT ($\leqslant$15 km) are considered. The black line is the mean of those profiles in COLs that are recognized at a certain level, and the grey line is the mean of the rest of the profiles. Error bars show $\pm\sigma$ from the mean. The red line means the two profiles are significantly different (statistically significant at the 95% confidence level, based on the Student's *t*-test). (a) The COLs recognized at 500 hPa. The mean LRT height of the 11 in-COL profiles is 10.3 km, and the mean LRT height of the other 72 profiles is 11.9 km. (b) The COLs recognized at 300 hPa. The mean LRT height of the 15 in-COL profiles is 10.5 km, and the mean LRT height of the other 68 profiles is 11.9 km. (c) The COLs recognized at 250 hPa. The mean LRT height of the 14 in-COL profiles is 10.5 km, and the mean LRT height of the other 69 profiles is 11.9 km. (d) The COLs recognized at 200 hPa. The mean LRT height of the 9 in-COL profiles is 10.8 km, and the mean LRT height of the other 74 profiles is 11.8 km. Panels (e–h) are similar to (a–d) but for the DT coordinate.

stability of in-COL profiles (red line) is 5.8×10^{-4} s^{-2}, while that of other profiles (black line) is 7.4×10^{-4} s^{-2}, indicating that the in-COL N^2 profiles around the tropopause are not as sharp as in normal profiles. This suggests that COLs may blur the barrier of the thermal tropopause and make it easier for STE to occur. In Fig. 10d, profiles are shown in the DT

coordinate. The characteristics of the profiles in the DT coordinate are similar to those of the LRT tropopause, except that the transition of static stability around the DT altitude is not as sharp as that around the LRT altitude.

Considering an area may stay under the control of a COL for a few days, the impact of the system in the area may begin before it has reached and continue after it has left. Thus, the 83 subtropical profiles were divided into four types according to the stage of the COL passing over Changchun: in-COLs, -1 day (one day before the COL); $+1$ day (one day after the COL); and others (normal profiles). In Fig. 10b, the in-COLs ozone profile (red line) exceeds the normal profile (black line) between more than ± 5 km around the tropopause. From 2 km below the tropopause to 5 km above, the $+1$ day profile (blue line) and -1 day profile (green line) also overlaps the normal profile. This is because, before a COL controls Changchun, the trough in front of the COL may transfer high ozone concentrations as well. When the COL system passes by Changchun, the ozone-rich mass still stays in the UTLS for more than one day. The high ozone concentration residence time may be related to the movement speed of the COL. We conclude that, on average, a substantial increase in ozone concentration in the UTLS occurs before the COL arrives, and lasts at least one day after the COL leaves.

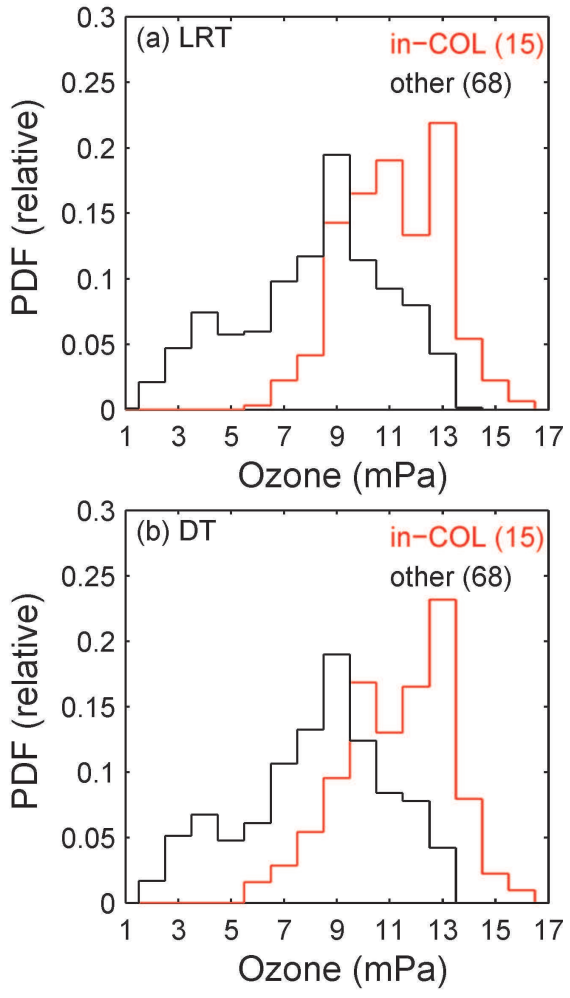

Fig. 9. (a) PDF of ozone at 1–3 km above the first LRT altitude for in-COL (300 hPa) profiles and other profiles. (b) As in (a) but above the DT altitude. The number of profiles for each group is shown in brackets behind the name of group. The HD in (a) and (b) is 0.47 and 0.48, respectively.

It is recognized from Fig. 3 that the increasing ozone concentration around the tropopause is accompanied by a descending of the tropopause. Knowing that COLs increase the ozone concentration in the LS (shown in Figs. 8 and 9), we therefore suggest that the increments of ozone concentration over Changchun may be related to COL strength. Hoskins et al. (1985) indicated that, in vertical cross sections through COLs, the PV above the tropopause becomes enhanced with the tropopause descent, and explained it using theoretical examples. Thus, to some extent, an increase in the PV value and a decrease in the tropopause height could indicate a COL's regional intensity. To test this notion, we analyzed the correlation between tropopause height and LS column ozone. In Figs. 10c and f, the LS column ozone in COLs possesses a negative relationship with the LRT/DT height, with a coefficient of $-0.62/-0.55$ (statistically significant at the 95% confidence level, based on the Student's t-test). This negative correlation shows that there is a positive correlation between the intensity of COLs and LS ozone. These results support the view that the ozone concentration increase in the LS is impacted upon by the COL's intensity.

4. Summary

This paper presents a study of the increase in the UTLS ozone concentration caused by COLs, achieved by analyzing ozonesonde observations over Changchun, China, made during the summers of 2010 to 2012. We compared the mean ozone profile in May, June and July from 2010 to 2012, between Changchun and Sapporo, Japan. The ozone profile for Changchun shows a similar structure with that in Sapporo, but has a higher ozone concentration. The PDF of ozone in the 12–15 km region over Changchun shows a bimodal structure with peaks at 3 mPa and 9 mPa, whereas the PDF for Sapporo has a single peak at 2 mPa. Besides, there are more LRTs lower than 12 km over Changchun than over Sapporo. These results imply that Changchun is influenced more by polar air masses with high ozone concentrations, compared to Sapporo.

The average height of the thermal tropopause over Changchun is 12.0 km. The DTs defined by 3.5 PVU agree with most of the LRTs, except the tropical LRTs. The ozone time–height cross sections summarize all the profiles and clearly display the variations of the ozone vertical distribution. This analysis provides direct evidence of stratospheric subsidence. The PDFs of ozone at 1–3 km above the LRTs are quite different, with a DH of 0.62, between the profiles with subtropical LRTs and those with tropical LRTs. The ozone peak in PDFs influenced by tropical air masses is only 4 mPa, while the peak influenced by polar air masses is 9 mPa. On the other hand, the difference between ozone PDFs of double LRTs and single LRTs is not so significant, with

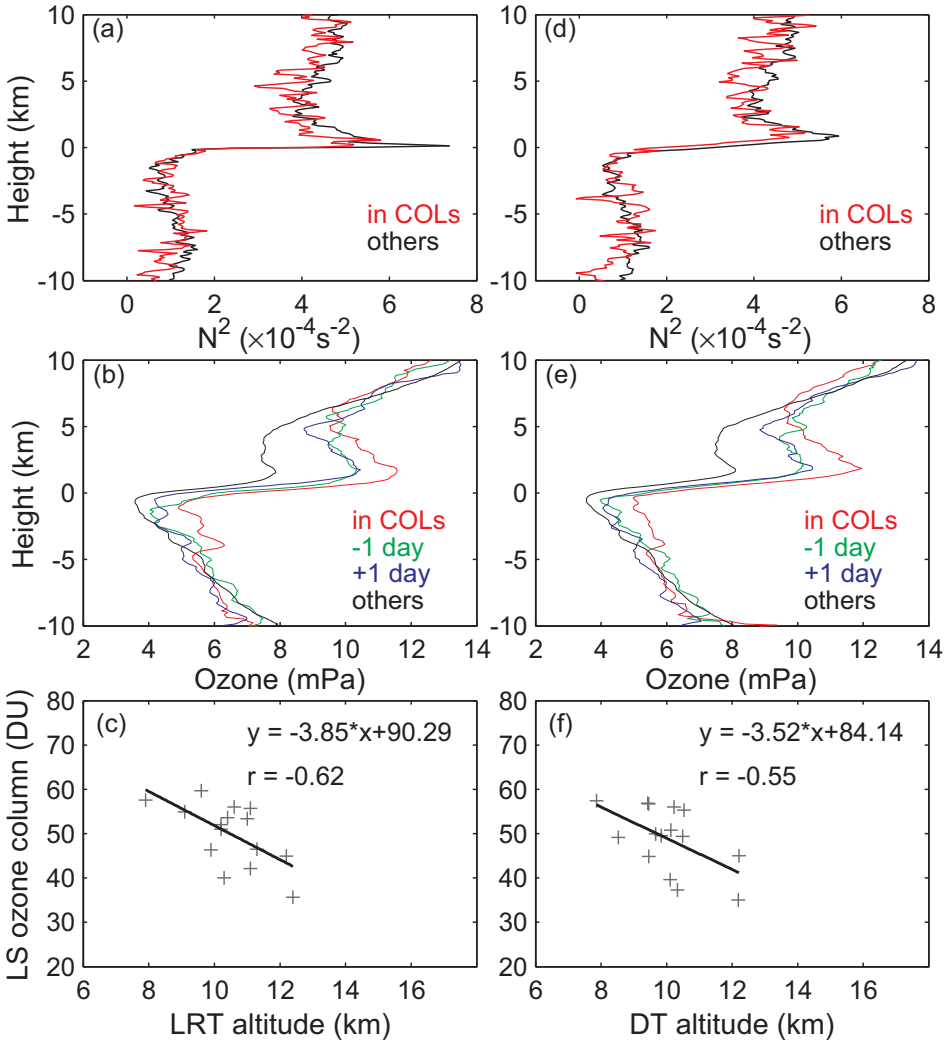

Fig. 10. (a) Composite static stability profiles in the LRT coordinate. The classification is based on whether there is a COL over Changchun at 300 hPa. The red (black) line marks the composite static stability of 15 profiles in COLs (68 profiles of others). (b) Composite ozone profiles in the LRT coordinate when Changchun is in four stages. The red line marks the composite of the 15 ozone profiles when Changchun had lows at 300 hPa. The green (blue) line marks the composite of six (ten) profiles at one day before (after) the low passed over Changchun. The black line marks the composite of the remaining 52 profiles, which are also called "normal" profiles. (c) Correlation between the height of the tropopause and the ozone column in the LS from 4 km below the LRT to the (LRT) of the 15 profiles in the COLs. The correlation coefficient is −0.62. Panels (d–f) are the same as (a–c) but in the DT coordinate.

an HD of 0.21. This is because a double tropopause can be caused by both stratospheric and tropospheric intrusion. It is also recognized that, when COLs remain over Changchun, the high ozone concentration in the stratosphere is transported downward. The tropopause in COLs is lowered. The air mass in COLs contains the high-ozone air from Siberia and the relatively lower ozone air from westerlies, without completely mixing. In most cases, Changchun is influenced by the high ozone concentration carried by COLs. Besides, the discussion on the ozone profile and static stability profile during a special case provided a picture of the STE process in different stages of COLs. A mature COL may convey ozone downwards and lower the tropopause. Later, in the decaying stage of the COL, the air mass transferred from the stratosphere at first acquires the tropospheric thermal characteristic, i.e., less stable (the DT could be 1.9 km lower than the LRT in the COL), and then gradually loses its high ozone concentration in the UTLS.

All of the 83 ozone profiles with a subtropical tropopause were classified into two types (in-COL profiles and other profiles), for investigating the relationship between COLs and the ozone concentration in the UTLS from a statistical perspective. The discrepancy between the two types of ozone profiles indicates that COLs may cause the ozone concen-

tration to increase between ± 4 km around the tropopause, and induce air masses that are less stable at 0–2 km above the tropopause. COLs may cause air to be less stable around the tropopause, and thus it is easier for STE to take place in such a system. On average, COLs lower the LRT height by 1.4 km, and the DT height by 1.7 km. Besides, the LS column ozone is 33% higher in COLs than other profiles. The PDFs of ozone at 1–3 km above the LRT, with an HD value of 0.47, also support the finding that the LS ozone in COLs is significantly higher than the LS ozone of other profiles. In addition, by analyzing the composite profiles of different stages, we investigated the time span of COLs' impacts on UTLS ozone. The results showed that the ozone concentration in the UTLS is impacted upon by COLs one day before the COL arrives. Moreover, the high ozone concentration is still observed in the UTLS one day after the COL has left. Lastly, we used the tropopause height as an indicator of COL strength over Changchun and found a negative relationship between the LRT/DT height and LS column ozone, with a coefficient of $-0.62/-0.55$, implying a positive relationship between COL strength and LS column ozone.

This study is based on the analysis of ozonesonde data and proves the impact of COLs on ozone in the UTLS from a statistical perspective. To further comprehend the details of the STE mechanisms at work in COLs, such as convection and tropopause folding, numerical model simulations would be an effective tool and an important supplement to our future investigations.

Acknowledgements. We thank Yuejian XUAN for his contribution to ozonesonde development, calibration and observation. We are grateful to Xiaowei WAN, Jinqiang ZHANG, Zhixuan BAI, and Chao LING for their contributions to the ozonesonde observations. We also acknowledge the NOAA for providing the HYSPLIT model, the ECMWF for providing the ERA-Interim reanalysis data, and the WOUDC for providing the ozonesonde data for Sapporo. This work was jointly supported by the National Basic Research Program of China (Grant No. 2010CB428602) and the National Natural Science Foundation of China (Grant Nos. 41275046 and 41025017).

REFERENCES

Barré, J., V. H. Peuch, J. L. Attié, L. El Amraoui, W. A. Lahoz, B. Josse, M. Claeyman, and P. Nédélec, 2012: Stratosphere-troposphere ozone exchange from high resolution MLS ozone analyses. *Atmospheric Chemistry and Physics*, **12**(14), 6129–6144.

Bethan, S., G. Vaughan, and S. J. Reid, 1996: A comparison of ozone and thermal tropopause heights and the impact of tropopause definition on quantifying the ozone content of the troposphere. *Quart. J. Roy. Meteor. Soc.*, **122**(532), 929–944.

Bian, J. C., 2009: Recent Advances in the study of atmospheric vertical structures in upper troposphere and lower stratosphere. *Advances in Earth Science*, **24**(3), 229–241. (in Chinese)

Bian, J. C., A. Gettelman, H. B. Chen, and L. L. Pan, 2007: Validation of satellite ozone profile retrievals using Beijing ozonesonde data. *J. Geophys. Res.*, **112**(D6), D06305, doi: 10.1029/2006JD007502.

Birner, T., A. Dörnbrack, and U. Schumann, 2002: How sharp is the tropopause at midlatitudes? *Geophys. Res. Lett.*, **29**(14), 45-1–45-4.

Bourqui, M. S., 2006: Stratosphere-troposphere exchange from the Lagrangian perspective: A case study and method sensitivities. *Atmospheric Chemistry and Physics*, **6**(9), 2651–2670.

Brewer, A. W., 1949: Evidence for a world circulation provided by the measurements of helium and water vapour distribution in the stratosphere. *Quart. J. Roy. Meteor. Soc.*, **75**(326), 351–363.

Chen, D., D. R. Lü, and Z. Y. Chen, 2014: Simulation of the stratosphere-troposphere exchange process in a typical cold vortex over Northeast China. *Science China Earth Sciences*, **57**(7), 1452–1463.

Cui, H., C. S. Zhao, Y. Qin, X. D. Zheng, Y. G. Zheng, C. Y. Chan, and L. Y. Chan, 2004: An estimation of ozone flux in a stratosphere-troposphere exchange event. *Chinese Science Bulletin*, **49**(2), 167–174.

Danielsen, E. F., R. S. Hipskind, S. E. Gaines, G. W. Sachse, G. L. Gregory, and G. F. Hill, 1987: Three-dimensional analysis of potential vorticity associated with tropopause folds and observed variations of ozone and carbon monoxide. *J. Geophys. Res.*, **92**(D2), 2103–2111.

Draxler, R. R., and G. D., Rolph, 2003: HYSPLIT (HYbrid Single-Particle Lagrangian Integrated Trajectory) model access via NOAA ARL READY website. NOAA Air Resources Laboratory, Silver Spring, MD. [Available online at http://www.arl.noaa.gov/ready/hysplit4.html]

Fishman, J., A. E. Wozniak, and J. K. Creilson, 2003: Global distribution of tropospheric ozone from satellite measurements using the empirically corrected tropospheric ozone residual technique: Identification of the regional aspects of air pollution. *Atmospheric Chemistry and Physics*, **3**(4), 893–907.

Ganguly, N. D., and C. Tzanis, 2011: Study of Stratosphere-troposphere exchange events of ozone in India and Greece using ozonesonde ascents. *Meteorological Applications*, **18**(4), 467–474.

Gettelman, A., P. Hoor, L. L. Pan, W. J. Randel, M. I. Hegglin, and T. Birner, 2011: The extratropical upper troposphere and lower stratosphere. *Reviews of Geophysics*, **49**(3), doi: 10.1029/2011RG000355.

Gimeno, L., R. M. Trigo, P. Ribera, and J. A. García, 2007: Editorial: Special issue on cut-off low systems (COL). *Meteor. Atmos. Phys.*, **96**(1–2), 1–2.

Gouget, H., G. Vaughan, A. Marenco, and H. G. J. Smit, 2000: Decay of a cut-off low and contribution to stratosphere-troposphere exchange. *Quart. J. Roy. Meteor. Soc.*, **126**(564), 1117–1141.

Holton, J. R., 1990: On the global exchange of mass between the stratosphere and troposphere. *J. Atmos. Sci.*, **47**(3), 392–395.

Homeyer, C. R., K. P. Bowman, and L. L. Pan, 2010: Extratropical tropopause transition layer characteristics from high-resolution sounding data. *J. Geophys. Res.*, **115**(D13), doi: 10.1029/2009JD013664.

Hoskins, B. J., M. E. McIntyre, and A. W. Robertson, 1985: On the use and significance of isentropic potential vorticity maps. *Quart. J. Roy.Meteor. Soc.*, **111**(470), 877–946.

Hu, K. X., R. Y. Lu, and D. H. Wang, 2010: Seasonal climatology of cut-off lows and associated precipitation patterns over Northeast China. *Meteor. Atmos. Phys.*, **106**(1–2), 37–48.

IPCC, 1996: Contribution of Working Group I to the Second Assessment Report of the Intergovernmental Panel on Climate Change, section 2. *Climate Change 1995-The Science of Climate Change*, J. T. Houghton et al., Eds., Cambridge University Press, 572 pp.

Kentarchos, A. S., and T. D. Davies, 1998: A climatology of cut-off lows at 200 hPa in the Northern Hemisphere, 1990–1994. *International Journal of Climatology*, **18**(4), 379–390.

Kim, J. H., and H. Lee, 2010: What causes the springtime tropospheric ozone maximum over Northeast Asia? *Adv. Atmos. Sci.*, **27**(3), 543–551, doi: 10.1007/s00376-009-9098-z.

Komhyr, W. D., R. A. Barnes, G. B. Brothers, J. A. Lathrop, and D. P. Opperman, 1995: Electrochemical concentration cell ozonesonde performance evaluation during STOIC 1989. *J. Geophys. Res.*, **100**(D5), 9231–9244.

Kuang, S., M. J. Newchurch, J. Burris, L. H. Wang, K. Knupp, and G. Y. Huang, 2012: Stratosphere-to-troposphere transport revealed by ground-based lidar and ozonesonde at a midlatitude site. *J. Geophys. Res.: Atmospheres*, **117**(D18), D18305, doi: 10.1029/2012JD017695.

Lefohn, A. S., H. Wernli, D. Shadwick, S. Limbach, S. J. Oltmans, and M. Shapiro, 2011: The importance of stratospheric–tropospheric transport in affecting surface ozone concentrations in the western and northern tier of the United States. *Atmos. Environ.*, **45**(28), 4845–4857.

Li, D., J. C. Bian, and Q. J. Fan, 2015: A deep stratospheric intrusion associated with an intense cut-off low event over East Asia. *Science China Earth Sciences*, **58**(1), 116–128.

Lin, M. Y., and Coauthors, 2012: Springtime high surface ozone events over the western United States: Quantifying the role of stratospheric intrusions. *J. Geophys. Res.*, **117**(D21), D00V22, doi: 10.1029/2012JD018151.

Liu, C. X., Y. Liu, X. Liu, and K. Chance, 2013: Dynamical and chemical features of a cutoff low over northeast China in July 2007: Results from satellite measurements and reanalysis. *Adv. Atmos. Sci.*, **30**(2), 525–540, doi: 10.1007/s00376-012-2086-8.

Logan, J. A., 1999a: An analysis of ozonesonde data for the lower stratosphere: Recommendations for testing models. *J. Geophys. Res.*, **104**(D13), 16151–16170.

Logan, J. A., 1999b: An analysis of ozonesonde data for the troposphere: Recommendations for testing 3-D models and development of a gridded climatology for tropospheric ozone. *J. Geophy. Res.*, **104**(D13), 16115–16149.

Mauzerall, D. L., D. Narita, H. Akimoto, L. Horowitz, S. Walters, D. A. Hauglustaine, and G. Brasseur, 2000: Seasonal characteristics of tropospheric ozone production and mixing ratios over East Asia: A global three-dimensional chemical transport model analysis. *J. Geophys. Res.*, **105**(D14), 17895–17910.

Nieto, R., and Coauthors, 2005: Climatological features of cutoff low systems in the northern hemisphere. *J. Climate*, **18**(6), 3085–3103.

Nikulin, M. S., 2001: Hellinger distance. *Encyclopeadia of Mathematics*. Ulf Rehmann et al., Eds., Springer. [Available online at http://www.encyclopediaofmath.org/index.php?title=h/h046890]

Ojha, N., and Coauthors, 2014: On the processes influencing the vertical distribution of ozone over the central Himalayas: Analysis of yearlong ozonesonde observations. *Atmos. Environ.*, **88**, 201–211.

Oltmans, S. J., and Coauthors, 1996: Summer and spring ozone profiles over the North Atlantic from ozonesonde measurements. *J. Geophys. Res.*, **101**(D22), 29179–29200.

Pan, L. L., W. J. Randel, B. L. Gary, M. J. Mahoney, and E. J. Hintsa, 2004: Definitions and sharpness of the extratropical tropopause: A trace gas perspective. *J. Geophys. Res.*, **109**(D23), D23103, doi: 10.1029/2004JD004982.

Pan, L. L., and Coauthors, 2007: Chemical behavior of the tropopause observed during the Stratosphere-Troposphere Analyses of Regional Transport experiment. *J. Geophys. Res.*, **112**(D18), 893–907, doi: 10.1029/2007JD008645.

Pan, L. L., and Coauthors, 2009: Tropospheric intrusions associated with the secondary tropopause. *J. Geophys. Res.*, **114**(D10), doi: 10.1029/2008JD011374.

Pittman, J. V., and Coauthors, 2009: Evaluation of AIRS, IASI, and OMI ozone profile retrievals in the extratropical tropopause region using in situ aircraft measurements. *J. Geophys. Res.*, **114**(D24), D24109, doi: 10.1029/2009JD012493.

Price, J. D., and G. Vaughan, 1993: The potential for stratosphere-troposphere exchange in cut-off-low systems. *Quart. J. Roy.Meteor. Soc.*, **119**(510), 343–365.

Randel, W. J., D. J. Seidel, and L. L. Pan, 2007: Observational characteristics of double tropopauses. *J. Geophys. Res.*, **112**(D7), doi: 10.1029/2006JD007904.

Srivastava, S., S. Lal, M. Naja, S. Venkataramani, and S. Gupta, 2012: Influence of regional pollution and long range transport over western India: Analysis of ozonesonde data. *Atmos. Environ.*, **47**, 174–182.

Sun, L., X. Y. Zheng, and Q. Wang, 1994: The climatological characteristics of northeast cold vortex in China. *Quarterly Journal of Applied Meteorology*, **5**(3), 297–303. (in Chinese)

Tilmes, S., and Coauthors, 2012: Technical Note: Ozonesonde climatology between 1995 and 2011: Description, evaluation and applications. *Atmospheric Chemistry and Physics*, **12**(16), 7475–7497.

Wang, G. C., Q. X. Kong, H. B. Chen, Y. J. Xuan, and X. W. Wan, 2004b: Characteristics of ozone vertical distribution in the atmosphere over Beijing. *Advance in Earth Science*, **19**(5), 743–748. (in Chinese)

Wang, G. C., Q. X. Kong, Y. J. Xuan, X. W. Wan, H. B. Chen, S. Q. Ma, and Q. Zhao, 2004a: Preliminary analysis on parallel comparison of GPSO3 and Vaisala ozonesondes. *J. Appl. Meteor. Sci.*, **15**(6), 672–680. (in Chinese)

Wang, Y., and Coauthors, 2012: Tropospheric ozone trend over Beijing from 2002–2010: Ozonesonde measurements and modeling analysis. *Atmospheric Chemistry and Physics*, **12**(18), 8389–8399.

Wirth, V., 1995: Diabatic heating in an axisymmetric cut-off cyclone and related stratosphere-troposphere exchange. *Quart. J. Roy. Meteor. Soc.*, **121**(521), 127–147.

WMO, 1957: Meteorology: A three-dimensional science: Second session of the Commission for Aerology. *WMO Bull.*, **6**, 134–138.

Xie, F. Q., and X. H. Cai, 2000: Spatial and temporal variation of total ozone over East-Asia. *Acta Scientiae Circumstantiae*, **20**(5), 513–517. (in Chinese)

Xuan, Y. J., S. Q. Ma, H. B. Chen, G. C. Wang, Q. X. Kong, Q. Zhao, and X. W. Wan, 2004: Intercomparisons of GPSO3 and Vaisala ECC ozone sondes. *Plateau Meteorology*, **23**(3), 394–399. (in Chinese)

Yang, J., and D. R. Lü, 2003: A simulation study of Stratosphere-troposphere exchange due to Cut-off-low over Eastern Asia. *Chinese J. Atmos. Sci.*, **27**(6), 1031–1044. (in Chinese)

Yates, E. L., and Coauthors, 2013: Airborne observations and modeling of springtime stratosphere-to-troposphere transport over California. *Atmospheric Chemistry and Physics*, **13**(24), 12 481–12 494.

Zhang, J. Q., Y. J. Xuan, X. L. Yan, M. Y. Liu, H. M. Tian, X. A. Xia, L. Pang, and X. D. Zheng, 2014a: Development and preliminary evaluation of a double-cell ozonesonde. *Adv. Atmos. Sci.*, **31**(4), 938–947, doi: 10.1007/s00376-013-3104-1.

Zhang, J. Q., Y. J. Xuan, X. A. Xia, M. Y. Liu, X. L. Yan, L. Pang, Z. X. Bai, and X. W. Wan, 2014b: Performance evaluation of a Self-developed ozonesonde and its application in an intensive observational campaign. *Atmos. Oceanic Sci. Lett.*, **7**(3), 175–179.

Zhang, M., W. S. Tian, L. Chen, and D. R. Lü, 2010: Cross-tropopause mass exchange associated with a tropopause fold event over the northeastern Tibetan Plateau. *Adv. Atmos. Sci.*, **27**(6), 1344–1360, doi: 10.1007/s00376-010-9129-9.